Supporting Information

A dinuclear Co(III)/Co(II) complex based on H_2pmide ligand showing field-induced SMM behaviour

Daiana Cabrosi[a], Carlos Cruz [b],[c], Verónica Paredes-García[b],[c] and Pablo Alborés[a]*

[a] Departamento de Química Inorgánica, Analítica y Química Física/ INQUIMAE (CONICET), Facultad de Ciencias Exactas y Naturales Universidad de Buenos Aires, Pabellón 2, Ciudad Universitaria, C1428EHA Buenos Aires, Argentina
Fax: +5411 / 4576-3341
E-mail: albores@qi.fcen.uba.ar

[b] Departamento de Ciencias Químicas, Facultad de Ciencias Exactas, Universidad Andres Bello, Avenida República 275, Santiago de Chile, Chile.

[c] Centro para el Desarrollo de la Nanociencia y Nanotecnología, CEDENNA, Santiago, Chile.

Table S1. Crystallographic data of complex **1**.

Empirical Formula	$C_{25}\ H_{43}\ Co_2\ N_2\ O_9$
Formula weight	633.5
T (K)	293 (2)
Crystal system	monoclinic
Space Group	$P2_1/n$
a (Å)	13.6175(5)
b (Å)	11.0711(3)
c (Å)	20.4071(7)
α (°)	90
β (°)	105.529(3)
γ (°)	90
V (Å^3)	2964.29(17)
Z	3
D_{calc} (mg/m^3)	1.419
Absorption coefficient (mm^{-1})	1.169
F(000)	1332
λ(Å)	0.71073
θ Range data collection (°)	3.4 – 27.0
Index ranges	$-17 \leq h \leq 15$
	$-13 \leq k \leq 14$
	$-25 \leq l \leq 25$
Reflections collected/unique	18833/ 6367
R_{int}	0.0486
Observed reflections [$I>2\sigma(I)$]	4583
Completeness (%)	99.7
Maximum / minimum transmission	0.91404/ 1.00000
Data/restraints/parameters	6367/180/352
Goodness-of-fit (GOF) on F^2	1.047
Final R-index [$I>2\sigma$(I)]/ all data	0.0661/ 0.0934
wR index [$I>2\sigma(I)$] /all data	0.1935/ 0.2214
Largest peak and hole (e A^{-3})	1.889 and -1.755
Weights, w	$1/[\sigma^2(F_o^2) + (0.1118P)^2 + 8.4195P]$ where $P=(F_o^2+2F_c^2)/3$

Table S2. Main bond lengths (Å) and angles (º) of complex **1**.

Co2	O5	2.065(4)
Co2	O2	2.100(4)
Co2	O1	2.090(4)
Co2	O4	2.089(4)
Co2	O7	2.019(4)
Co2	O3	2.225(5)
Co1	O1	1.897(4)
Co1	O2	1.901(4)
Co1	N2	1.937(4)
Co1	O8	1.919(5)
Co1	O6	1.916(4)
Co1	N1	1.932(4)
Co1	Co2	2.964(1)

O5	Co2	O7	94.7(2)
O5	Co2	O2	88.5(1)
O5	Co2	O1	86.1(1)
O5	Co2	O4	105.1(2)
O3	Co2	O7	86.6(2)
O3	Co2	O4	60.4(2)
O3	Co2	O1	95.6(2)
O3	Co2	O2	106.0(2)
N2	Co1	N1	85.0(2)
N2	Co1	O8	88.1(2)
N2	Co1	O2	85.6(2)
N2	Co1	O1	87.5(2)
O6	Co1	O8	94.0(2)
O6	Co1	N1	92.9(2)
O6	Co1	O2	96.4(2)
O6	Co1	O1	90.3(2)
O6	Co1	N1	92.9(2)

Table S3. DFT-broken symmetry computed Mulliken spin density of complex **1** H-bonded dimeric unit.

	HS	BS
Co(II) sites	2.761161 / 2.761120	-2.761087 / 2.761052
O aqua ligands	0.029364 / 0.029375	-0.029511 / 0.029519
O pmide ligands	0.032986 / 0.032971	-0.032679 / 0.032666

Table S4. Complex **1** AC magnetic susceptibility data fitting parameters according to Debye model (see text).

T / K	χ_S / cm^{3}mol^{-1}	χ_T / cm^{3}mol^{-1}	α	τ / s
2	0.43	0.74	0.35	4.81E-05
2.2	0.4	0.7	0.33	4.98E-05
2.4	0.38	0.67	0.32	5.10E-05
2.6	0.35	0.63	0.31	5.07E-05

2.8	0.32	0.6	0.3	4.90E-05
3	0.3	0.57	0.28	4.70E-05
3.2	0.28	0.54	0.26	4.33E-05
3.5	0.26	0.5	0.25	3.97E-05
3.8	0.24	0.47	0.24	3.54E-05
4.1	0.22	0.45	0.23	3.15E-05
4.5	0.21	0.42	0.21	2.78E-05
4.9	0.19	0.39	0.18	2.47E-05
5.3	0.18	0.36	0.18	2.10E-05
5.7	0.17	0.34	0.15	1.86E-05
6.2	0.16	0.31	0.11	1.63E-05
6.7	0.15	0.29	0.08	1.35E-05
7.3	0.14	0.27	0.05	1.05E-05
7.9	0.13	0.25	0.03	7.58E-06
8.5	0.1	0.24	0.04	3.89E-06
9.2	0.09	0.22	0	2.14E-06
10	0.08	0.21	0	9.78E-07

H / Oe	**$\Delta\chi_1$/ cm^{3}mol^{-1}**	**$\Delta\chi_2$ / cm^{3}mol^{-1}**	**χ_S/ cm^{3}mol^{-1}**	**α_1**	**τ_1/ s**	**α_2**	**τ_2/ s**
800	0.04	0.04	0.70	0.15	2.4e-4	5.7E-15	3.0E-6
1000	0.06	0.55	0.15	0.19	1.9E-4	1.5E-13	2.6E-6
1200	0.10	0.18	0.47	0.31	1.3E-4	0.10	6.8E-6

***H* / Oe**	**χ_S/ cm^{3}mol^{-1}**	**χ_T / cm^{3}mol^{-1}**	**α**	**τ/ s**
1600	0.43	0.73	0.33	5.71E-05
1800	0.43	0.7	0.30	6.78E-05
2000	0.44	0.68	0.29	7.94E-05
2200	0.44	0.66	0.28	9.23E-05
2400	0.42	0.63	0.24	9.62E-05
2600	0.39	0.61	0.24	9.74E-05
2800	0.34	0.59	0.26	9.22E-05
3000	0.29	0.56	0.25	8.75E-05

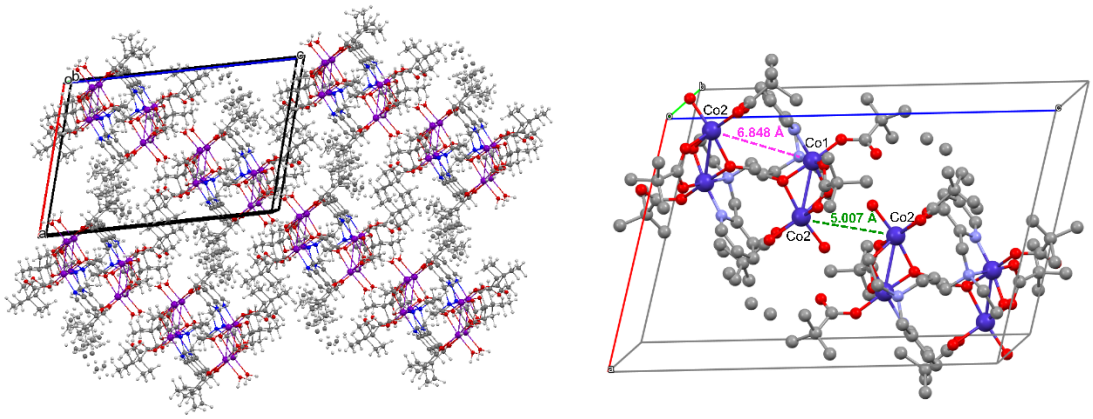

Figure S1. Complex **1** crystal structure molecular packing, view along *b*-axis (left); unit cell packing of two H-bond dimeric units (right).

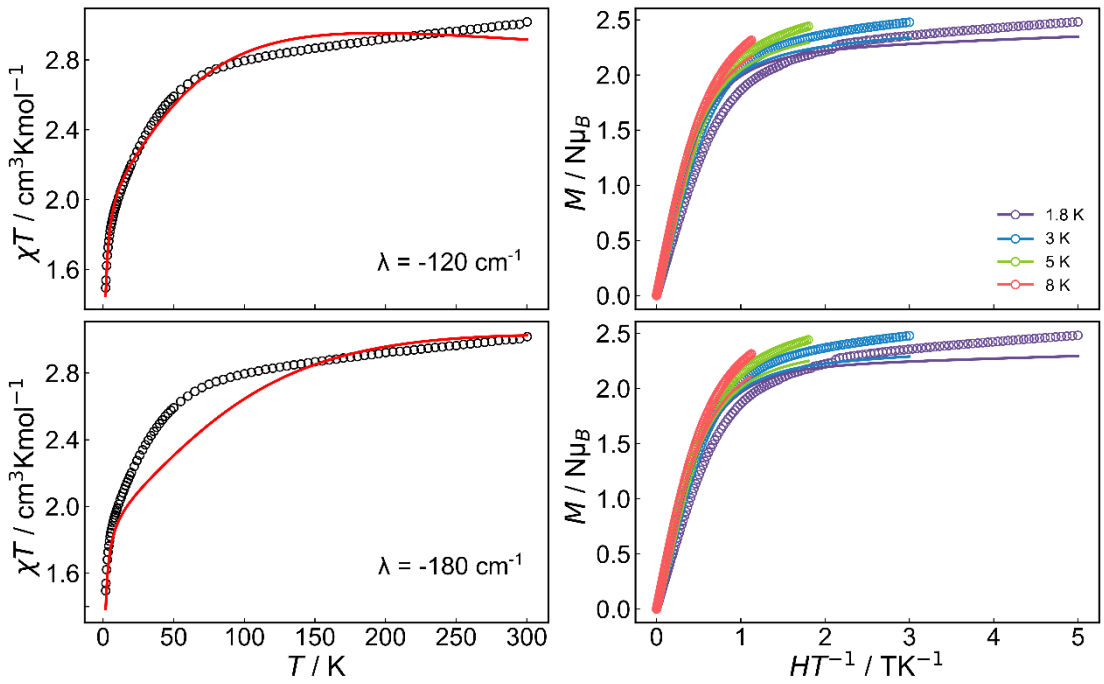

Figure S2. Magnetic susceptibility temperature dependence at 1000 Oe (left) and variable temperature reduced magnetization up to 90 kOe (right) of complex **1**. Open symbols: experimental; full line: best fitting according to Hamiltonian of Eq .2, see text for details.

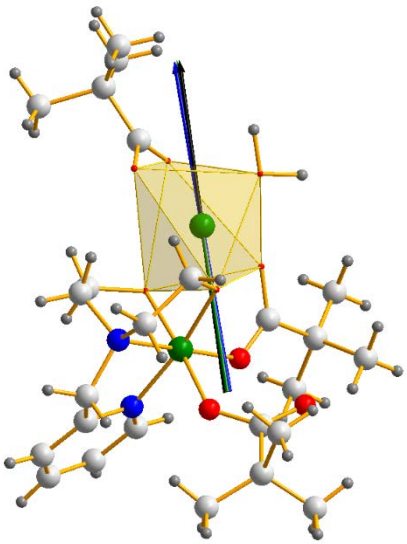

Figure S3. Complex **1** Co(II) site main axis orientation as arising from *ab-initio* computations; *D*-tensor (black), g tensor (blue) and ground state KD g tensor (green).

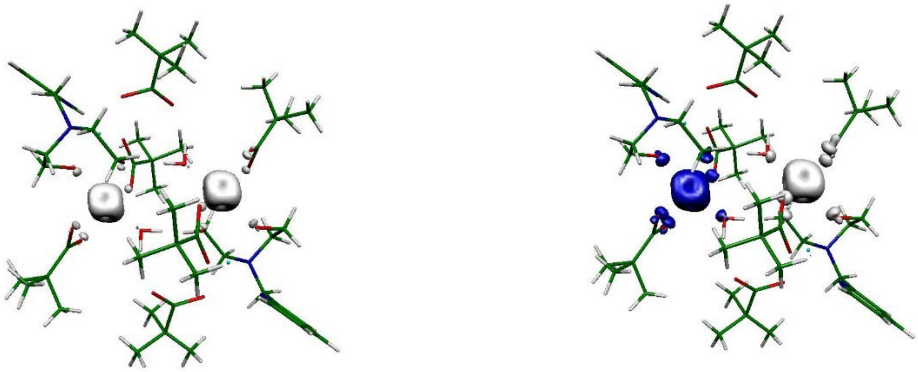

Figure S4. Spin density isosurfaces (0.02 a.u.) arising from BS-DFT computation of complex **1** H-bonded dimeric unit; High-spin (HS) left, Broken-Symmetry (BS), right.

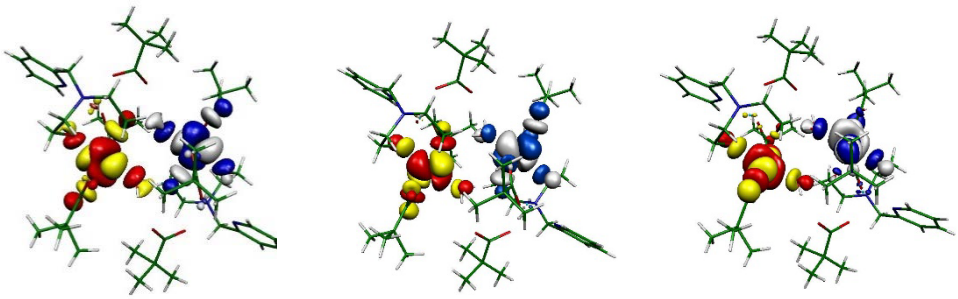

$S_{\alpha\beta}$	0.00768	0.00176	0.00017

Figure S5. Magnetic orbitals isosurfaces (0.02 a.u.) and overlap integral in terms of COT arising from BS-DFT computation of complex **1** H-bonded dimeric unit.

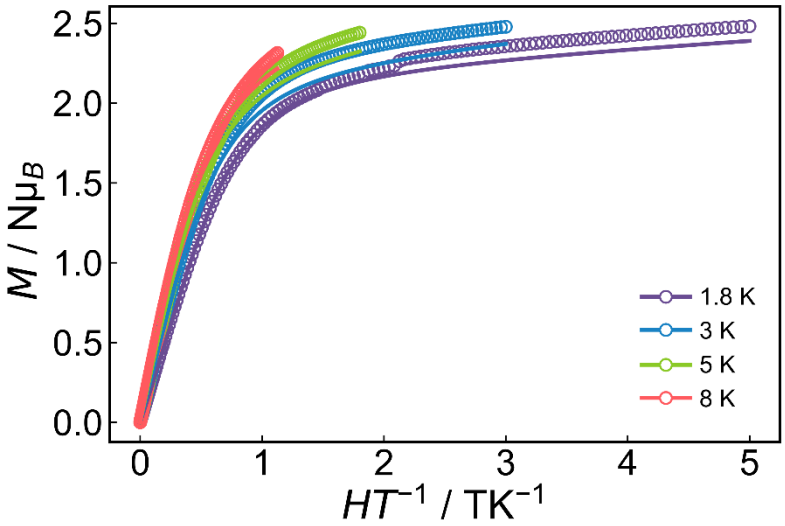

Figure S6. Variable temperature reduced magnetization up to 90 kOe (right) of complex **1**. Open symbols: experimental; full line: best fitting according to Hamiltonian of Eq .4, see text for details.

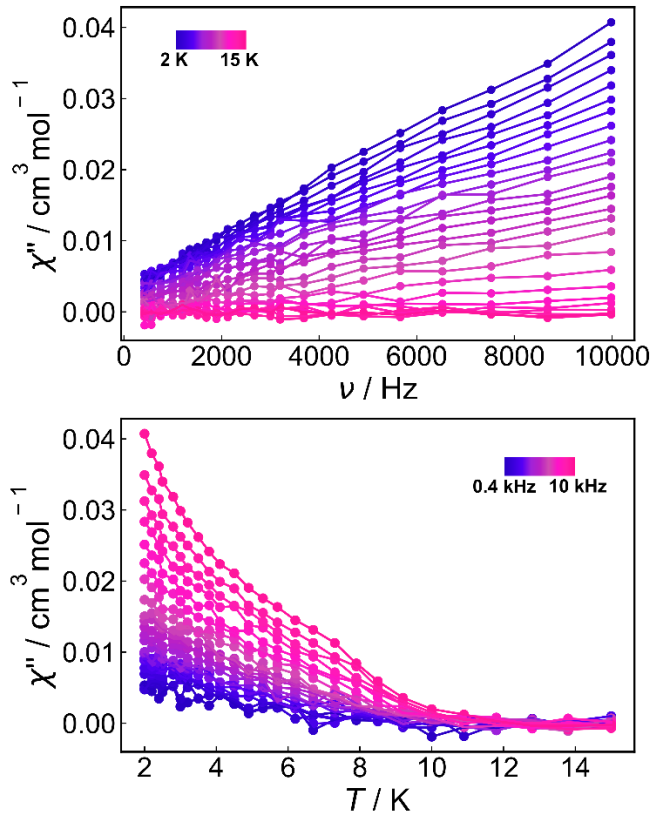

Figure S7. AC magnetic susceptibility of complex **1**. Variable temperature data at 300 Oe external DC field. Full symbols: experimental; full line: eye guideline.

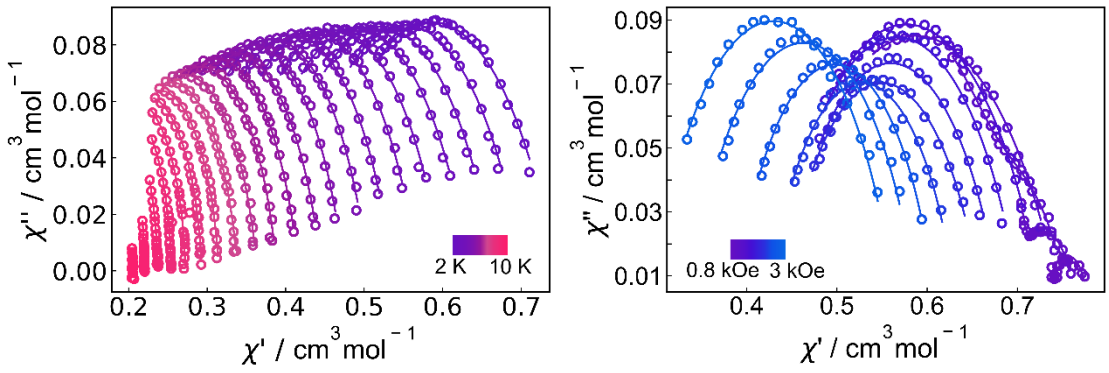

Figure S8. Cole-Cole plots of complex **1** AC magnetic susceptibility data. Temperature and frequency sweeping at 1500 Oe DC external field (left); external DC field sweeping at 2 K (right). Open symbols: experimental; full lines: simulated with best fitting parameters arising from the generalized Debye model (see text).

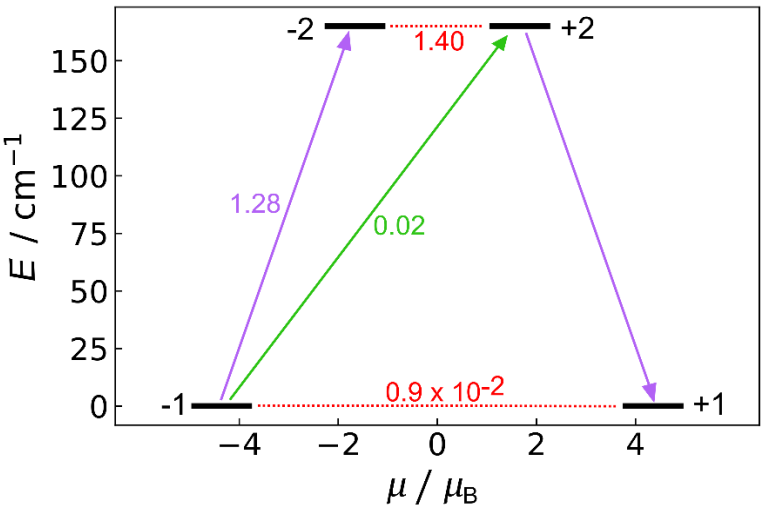

Figure S9. *Ab-initio* computed low lying energy levels (two lowest KDs) and transition moment matrix elements showing most probable magnetization relaxation pathway.

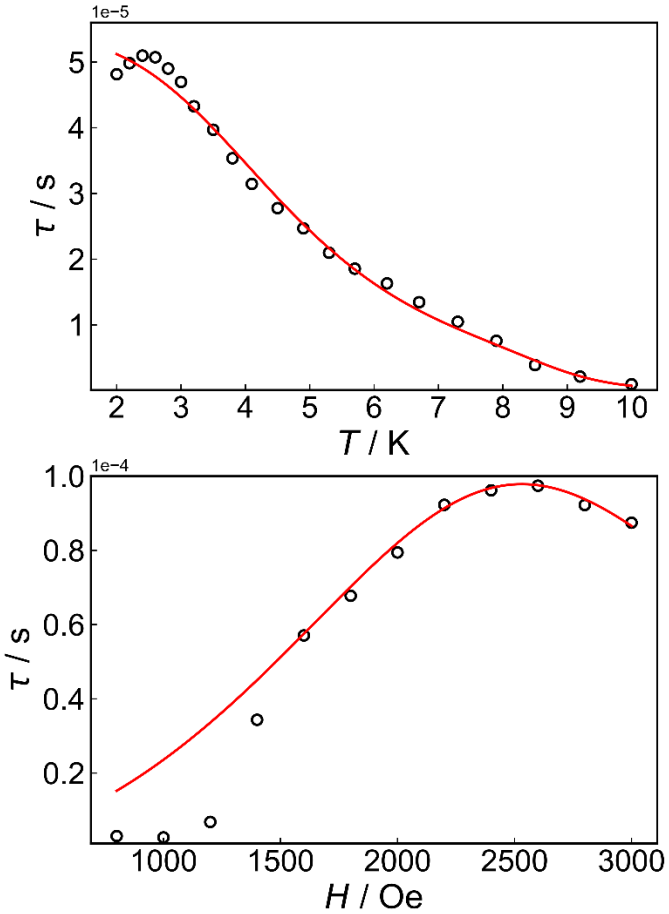

Figure S10. Complex **1** magnetization characteristic relaxation time temperature dependence at 1500 Oe DC external field (top) and field dependence at 2 K (bottom).

Open symbols: experimental; full line: simulation with best simultaneous fitting parameters according to Eq. 5 (see text for details).

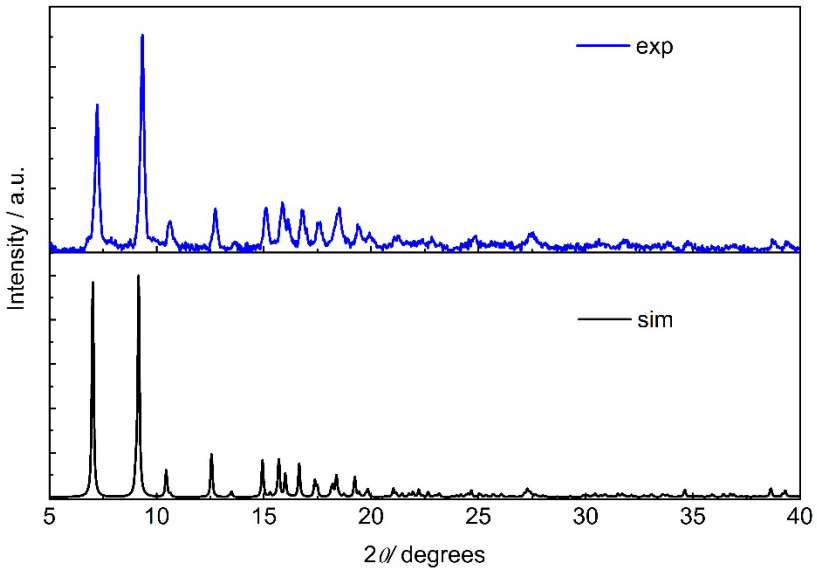

Figure S11. Powder X-ray diffractogram of complex **1** at room temperature. Top: experimental data; bottom: simulated data from single crystal X-ray refinement.